

Published in final edited form as:

Biochemistry. 2013 July 23; 52(29): . doi:10.1021/bi400338f.

Kinetic and Isotopic Characterization of *L*-Proline Dehydrogenase from *Mycobacterium tuberculosis*

Hector Serrano and John S. Blanchard*

Department of Biochemistry, Albert Einstein College of Medicine, 1300 Morris Park Avenue, Bronx, New York 10461

Abstract

The monofunctional proline dehydrogenase (ProDH) from *Mycobacterium tuberculosis* performs the flavin-dependent oxidation of *L*-proline to Δ^1 -pyrroline-5-carboxylate (P5C) in the proline catabolic pathway. The ProDH gene, *prub*, was cloned into the pYUB1062 vector, and the C-terminal His-tagged 37 kDa protein was expressed and purified by nickel-affinity chromatography. A steady-state kinetic analysis revealed a ping-pong mechanism with an overall k_{cat} of $33 \pm 2 \text{ sec}^{-1}$ and K_m values of $5.7 \pm 0.8 \text{ mM}$ and $3.4 \pm 0.3 \mu\text{M}$ for *L*-proline and 2,6-dichlorophenolindophenol (DCPIP), respectively. The pH dependence of k_{cat} revealed that one enzyme group exhibiting a pK value of 6.8 must be deprotonated for optimal catalytic activity. Site-directed mutagenesis suggests that this group is Lys110. The primary kinetic isotope effects on V/K_{Pro} and V of 5.5 and 1.1, respectively, suggest that hydride transfer from *L*-proline to FAD is rate-limiting for the reductive half-reaction, but that FAD reoxidation is the rate-limiting step in the overall reaction. Solvent and multiple kinetic isotope effects suggest that *L*-proline oxidation occurs in a stepwise rather than concerted mechanism. Pre-steady state kinetics reveal an overall k_{red} of $88.5 \pm 0.7 \text{ sec}^{-1}$, and this rate is subject to a primary kinetic isotope effect of 5.2. These data confirm that the overall reaction is limited by reduced flavin reoxidation in the second half-reaction.

Keywords

amino acid metabolism; kinetic analysis; kinetic isotope effects; tuberculosis

Mycobacterium tuberculosis (Mtb), the causative agent of tuberculosis (TB), is a global health concern [1]. In 2011, there were an estimated 8.7 million new cases of TB, with 1.4 million deaths from TB. In spite of research into the eradication of TB, the rise of drug-resistant strains of MTb are becoming alarming common, and new drug targets need to be discovered [2].

Recently, the oxidation of *L*-proline has come under scrutiny for its possible protection of *Mycobacterial* cells under hypoxic conditions [3, 4]. Berney and Cook observed an increase in the production of proline dehydrogenase (ProDH) at low $[O_2]$, and argued that the product of ProDH, Δ^1 -pyrroline-5-carboxylate (P5C), reacts with methylglyoxal, a toxic by-product of several metabolic pathways, to form 2-acetyl-1-pyrroline (2-AP) [5–9].

The oxidation of *L*-proline to *L*-glutamate follows a two-enzyme pathway with Δ^1 -pyrroline-5-carboxylate as an intermediate (Scheme 1). In most prokaryotes, the two enzymes, proline dehydrogenase (ProDH) and Δ^1 -pyrroline-5-carboxylate dehydrogenase

*To whom correspondence should be addressed: Department of Biochemistry, Albert Einstein College of Medicine, 1300 Morris Park Ave., Bronx, NY 10461. Phone: (718) 430-3096. Fax: (718) 430-8565. john.blanchard@einstein.yu.edu.

(P5CDH) are a single fused protein, named proline utilization A (PutA), while in eukaryotes and some prokaryotes they are separate enzymes [10]. The *L*-proline dehydrogenase activity of both the fused multifunctional and the mono-functional enzymes have been studied [11, 12]. Crystal structures have also been solved for both forms of the enzyme, suggesting two residues equivalent to K110 and Y203 in the Mtb ProDH, as potential active site bases [12, 13]. The flavin-dependent ProDH activity of PutA from *E. coli* was recently characterized, both in the steady- and pre-steady state [11, 14]. It was found to follow a two-site ping-pong mechanism utilizing various electron acceptors. Pre-steady state experiments allowed the k_{red} and k_{ox} rates of PutA of 38 sec⁻¹ and 7.5 sec⁻¹, respectively, to be determined. No studies of *Mycobacterium tuberculosis* ProDH have been reported to date, and we present here a kinetic and mechanistic analysis of the enzyme.

Materials and Methods

Materials

Chemicals, biochemicals, buffers, and solvents were purchased from Sigma-Aldrich Chemical Co. (St. Louis, MO) or Fisher Scientific Inc. (Pittsburgh, PA), unless stated otherwise. LB Broth, agar, Middlebrook 7H9 and BBL Middlebrook ADC Enrichment were obtained from Becton, Dickinson and Company (Franklin Lakes, NJ). Nucleic acid primers were from Invitrogen. The pET-29a(+) vector was from Novagen. The *Mycobacterium smegmatis* mc²4517 cells and pYUB1062 vector were a gift from William R. Jacobs Jr. (Einstein College of Medicine). Hygromycin B and Ni-NTA were purchased from Gold Biotechnology (St. Louis, Missouri). Enzymes, reagents and deoxynucleotide triphosphates (dNTPs) used for the cloning procedures were purchased from New England Biolabs (Ipswich, MA). 99.9% deuterated water was from Cambridge Isotope Laboratories (Andover, MA). [2,5,5-²H₃]-*L*-proline was from Medical Isotopes, Inc (Pelham, NH). Prepacked PD-10 Sephadex G-25 columns were purchased from GE Healthcare Lifesciences (Piscataway, NJ).

Cloning, Overexpression, and Purification of ProDH—The Mtb *prub* gene (Rv1188) was PCR amplified from Mtb H37Rv DNA using the forward primer 5'-ATCCCGCTCATATGGCCGGCTGGTTTCGCGCAC-3' and reverse primer 5'-ATCCCGCTAAGCTTGGCGCTCGGCGCACCCCCG-3'. Amplification mixtures contained the appropriate synthetic primers, deoxynucleotide triphosphates, genomic DNA, and PCR reagents. The resulting PCR product and the pET29a(+) vector were digested with *NdeI* and *HindIII* restriction enzymes, purified, and ligated using T4 DNA ligase. An aliquot of the ligation mixture was transformed into competent *E. coli* DH5 α cells. Transformants were selected at 37 °C on LB (10 g Bacto-tryptone, 5 g yeast extract, 10 g NaCl) plates with kanamycin (30 μ g/ml) for selection. Plasmid DNA was isolated from several randomly selected colonies and analyzed by restriction analysis for the presence of the insert. The cloned *prub* gene was sequenced to verify that no other mutations had been introduced during the amplification of the gene. The newly constructed expression vector was named pET29:*prub*.

Because of a lack of protein expression, the gene fragment was subcloned into the *mycobacterial* pYUB1062 expression vector using the same *NdeI* and *HindIII* restriction sites. After the sequence had been verified, the recombinant plasmid, pYUB1062:*prodh*, was transformed into *Mycobacterium smegmatis* mc²4517 cells. A single bacterial colony was selected and grown for 19 hr at 37°C in media containing 27 mL Middlebrook 7H9 broth medium supplemented with 3 mL of BBL Middlebrook ADC Enrichment, 0.05% Tween 80, 0.2% glycerol, kanamycin (20 μ g/ml), and hygromycin B (100 μ g/ml). Cells were then inoculated into 12 x 1L of the above medium and grown to mid-exponential phase (OD₆₀₀=

0.5–0.6) at 37°C before induction with acetamide (4 mL of a 0.5 g/mL solution made in water) and allowed to grow for 18 h. Cells were harvested by centrifugation, and the pellets were resuspended in cold 50 mM Tris (pH 8.0) containing 300 mM NaCl, 10 mM imidazole and 0.1% Triton X-100 (lysis buffer), lysed using an EmulsiFlex-C3 homogenizer (Avestin, Ottawa, Canada) and centrifuged at 17,000 rpm for 45 min to remove cellular debris. Batch purification was performed with a Ni-NTA agarose column. The column was washed with lysis buffer, and the protein was eluted with 250 mM imidazole in lysis buffer and stored at 4 °C.

K110A and Y203F ProDH Mutants—K110A and Y203F ProDH were prepared using overlap extension PCR [15]. The forward primer (5'-ATCCCGCTCATATGGCCGGCTGGTTTCGCGCAC-3') is designated primer F1 and contains an *NdeI* restriction site (underlined) followed by 18 bases corresponding to the coding sequence of the *prub* gene. The reverse primer (5'-ATCCCGCTAAGCTTCGCTCGGCGCACCCCG-3') is designated primer R1 and contains a *HindIII* restriction site (underlined) followed by 18 bases corresponding to the complementary sequence of the *prub* gene. The internal PCR primers for K110A were oligonucleotides 5'-GTGTCGCTCGCGCTGTCGGCGCTC-3' and 5'-GAGCGCCGACAGCGGAGCGACAC-3', where the mutated codons are in bold. The internal PCR primers for Y203F were oligonucleotides 5'-CAAGGGCGCCTTTGACGAACCCGC-3' and 5'-GCGGGTTCGTCAAAGGCGCCCTT-3', where the mutated codons are in bold. Expression, purification and storage of the mutant forms of the enzyme followed the same protocol that was used for the wild type.

Protein Concentration—The concentration of WT ProDH and the two mutants was determined spectrophotometrically using an ϵ_{451} of 11,300 M⁻¹ cm⁻¹.

Measurement of Enzymatic Activity—Unless otherwise stated, all steady-state kinetic assays were performed at 25 °C and pH 7.1 in 20 mM Tris-HCl. ProDH activity was assayed by measuring the reduction of the artificial electron acceptor 2,6-dichlorophenolindophenol (DCPIP). The reaction mixture was composed of 20 mM Tris-HCl, ProDH, DCPIP and *L*-proline in a total volume of 1 mL. The reaction was initiated by the addition of *L*-proline. Reactions were monitored spectrophotometrically until 10% substrate conversion to product. Rates were calculated using the molar extinction coefficient of DCPIP ($\epsilon_{600} = 18,700$ M⁻¹ cm⁻¹) and the total enzyme concentration (E_t).

Initial Velocity of WT, K110A and Y203F ProDH—Initial kinetic parameters were estimated by saturating with one substrate and varying the concentration of the other substrate. The resulting curve was fit to eq 1:

$$v = (V_{\max} * A) / (K_m + A) \quad (1)$$

where V_{\max} is the maximal velocity and A is the concentration of the varied substrate. Initial velocity studies were conducted at fixed, saturating concentrations of proline and varying concentrations of DCPIP and vice versa. The resulting patterns were fit globally to eq 2 for a ping-pong mechanism:

$$v = (VAB) / (K_a B + K_b A + AB) \quad (2)$$

where V is the maximal velocity, A and B are the substrate concentrations, and K_a and K_b are the respective Michaelis constants for each substrate.

pH Dependence of ProDH Activity—The pH dependencies of the kinetic parameters were determined in a mixed buffer solution (20 mM each MES, Bis-tris propane and CHES) at the desired pH under saturating conditions of DCPIP and varying concentrations of *L*-proline. The resulting k_{cat} and $k_{\text{cat}}/K_{\text{pro}}$ data were fit to eq 3:

$$\log k_{\text{cat}} \text{ or } \log k_{\text{cat}}/K_{\text{pro}} = \log C / (1 + [H^+]/K) \quad (3)$$

where C is the pH-independent plateau value, K is the observed dissociation constant for the ionizing group, and $[H^+]$ is the hydrogen ion concentration. This equation describes the pH dependence where the protonation of a single group decreases the magnitude of the kinetic parameter.

Primary Kinetic Isotope Effects—Assays were performed under saturating DCPIP conditions and varying concentrations of either *L*-proline or [2,5,5-²H₃]-*L*-proline in 20 mM tris-HCl pH 8.0, where the enzymatic rate is independent of pH. The results were globally fit to eq 4:

$$v = (VA) / (K(1 + F_i(E_{V/K} - 1)) + A(1 + F_i E_v - 1)) \quad (4)$$

where V is the maximal velocity, A is the concentration of *L*-proline or [2,5,5-²H₃]-*L*-proline, F_i is the fraction of isotope (0 or 0.982), $E_{V/K}$ is the effect on $k_{\text{cat}}/K_{\text{pro}}$, and E_v is the effect on k_{cat} .

Solvent Kinetic Isotope Effects—Solvent kinetic isotope effects were measured at saturating concentrations of DCPIP and varying concentrations of *L*-proline and globally fit to eq 4 where $F_i = 0$ for H₂O and $F_i = 0.92$ for D₂O. A viscosity control of 9% glycerol did not show any effect on either V or V/K_{pro} . A proton inventory was determined under saturating conditions of both DCPIP and *L*-proline at 10% increments from 0 to 90% of D₂O.

Stopped-Flow Measurements—All measurements were conducted on a SX-20 stopped-flow spectrophotometer operating in the absorbance mode at 451 nm (Applied Photophysics). Assays contained 14 μM ProDH (after mixing) and variable concentrations of *L*-proline or [2,5,5-²H₃]-*L*-proline, to ensure that binding is not contributing to the observed rates. Measurements were performed in 50 mM Tris-HCl (pH 8.4) containing 100 mM NaCl, 5 mM DTT and 5% glycerol made in water or D₂O. The reduction of flavin by substrate was monitored over time and fit to eq 5:

$$A = A_f + A_1 e^{-k_1 t} + A_2 e^{-k_2 t} \quad (5)$$

where A is the absorbance at time t , A_f is the final absorbance, and A_1 and A_2 are the absorbance changes associated with each of the first-order rate constants, k_1 and k_2 , respectively [16]

The k_{obs} values obtained at various concentrations of substrate were replotted as a function of enzyme concentration and fit to eq 6:

$$k_{\text{obs}} = (k_H S) / (K_d + S) \quad (6)$$

where k_{obs} is the observed rate constant after the single-exponential fitting at different concentrations of enzyme, k_H is the rate obtained with *L*-proline used as the substrate, S is the *L*-proline concentration, and K_d is the dissociation constant for *L*-proline. The isotope

effect on the hydride transfer step or proton extraction step (Dk_H) was obtained by dividing k_H/k_D , using the values obtained after fitting with eq 6.

Results and Discussion

Cloning, Expression and Purification

The *prub* gene was amplified from genomic DNA of *M. tuberculosis H37Rv* and fused into the start codon of expression vector pET29a(+), resulting in the pET29:*prub* construct. The construct was sequenced to verify that no mutation was introduced by PCR. The *prub* gene in pET29:*prub* is under the control of a T7 promoter, and expression of the enzyme was attempted in *E. coli* T7 express, with no success. The gene was then sub-cloned into the pYUB1062 vector, to generate pYUB1062:*prodh*, for protein expression. The K110A and Y203F mutants genes were amplified from the pYUB1062:*prodh* construct and sequenced to confirm only the designated mutant was introduced by PCR. Over-expression of the C-terminally His₆-tagged WT and mutant forms of the enzyme yielded soluble protein of the expected mass, ~37 kDa.

Initial velocity studies

The parallel initial velocity pattern obtained using *L*-proline and DCPIP (Figure 1), an artificial electron acceptor, reveals that ProDH exhibits a ping-pong kinetic mechanism, as observed for all other mono- and bi-functional proline dehydrogenases [11, 12, 14]. (Figure 1) A k_{cat} of $33 \pm 2 \text{ sec}^{-1}$ was determined. This value is similar to what was found for the *E. coli* ProDH measured with various other electron acceptors [11]. The K_m values for *L*-proline and DCPIP were $5.7 \pm 0.8 \text{ mM}$ and $3.4 \pm 0.3 \mu\text{M}$, respectively (Table 1).

pH dependence of the kinetic parameters

To probe the potential involvement of general acid or general base catalysis in the mechanism of ProDH, the pH dependencies of k_{cat} and k_{cat}/K_m were examined between pH 5.5 and 9.0, the range in which the enzyme was found to be stable. The pH profile was determined at a saturating concentration of DCPIP and varying concentrations of *L*-proline. The pH dependencies of k_{cat} and k_{cat}/K_{pro} are determined by a single ionizable group exhibiting pK_a values of 6.8 ± 0.1 and 7.1 ± 0.2 , respectively (Figure 2) that needs to be deprotonated for catalysis and binding. The k_{cat}/K_{pro} data at low pH values deviate somewhat from the fit to a single ionizable group, but clearly is not consistent with two ionizable groups that must be deprotonated (dashed line in Figure 2).

The crystal structure of *E. coli* PutA in complex with the competitive inhibitor, *L*-tetrahydro-2-furoic acid, provides clues into which residues could function as an active site base, Lys329 or Tyr437 [13]. In the active site, Tyr437 is hydrogen-bound to a water molecule, which is the closest neighbor to what would be the amine group of proline. The ϵ -amino group of Lys329 is 3.5 Å from *L*-tetrahydro-2-furoic acid, suggesting it could also play a role in catalysis. A more recent structure of the monofunctional ProDH from *Deinococcus radiodurans* similarly shows the ϵ -amino group of Lys98 (equivalent to K110 in the Mtb ProDH) is 3.5 Å from the ring oxygen atom of the same inhibitor [23]. Sequence alignments of the bifunctional *E. coli* PutA with the monofunctional ProDH's from *Deinococcus radiodurans*, *Thermus thermophilus*, *Mycobacterium smegmatis* and *Mycobacterium tuberculosis* shows both these residues, Lys110 and Tyr203 (Mtb numbering), are conserved in *Mycobacterium tuberculosis* ProDH (Figure 3). We therefore generated the K110A and Y203F mutant forms of the enzyme. The K110A mutant has no measurable catalytic activity, while the Y203F mutant exhibited an increase in the K_{pro} but no change in k_{cat} (Table 1). These data strongly argue that Y203 serves to bind and orient *L*-

proline in the active site, but that the active site base observed in the pH profile of k_{cat} is K110.

Steady-state Kinetic Isotope Effects

To investigate the rate-limiting nature of the catalytic oxidation of *L*-proline, primary kinetic isotope effects (KIEs) were measured at pH 8.1, using *L*-proline and [2,5,5- $^2\text{H}_3$]-*L*-proline as substrates (Figure 4A). Normal KIEs were observed with a very large primary effect on $^{\text{D}}V/K_{\text{pro}}$ of 5.6 ± 0.1 and a small effect on $^{\text{D}}V$ of 1.1 ± 0.2 . The equations that describe the V and V/K_{pro} isotope effects can be derived from the model shown in Scheme 2, neglecting any contribution from the reverse commitment factor. The commitment factor that determines the extent and degree to which the intrinsic primary kinetic isotope effect is observed for V/K_{pro} is k_3/k_2 , that is, the ratio of the rate of the chemical step defining the oxidation of *L*-proline to form Δ^1 -pyrroline-5-carboxylate divided by the rate of dissociation of *L*-proline from the binary Michaelis complex. The large size of $^{\text{D}}V/K_{\text{pro}}$ argues that chemistry is much slower than dissociation, and thus, *L*-proline is not a “sticky” substrate. The commitment factor for V for a ping-pong reaction sequence is k_3/k_7 , the ratio of the two chemical steps that result in enzyme-bound flavin reduction (k_3) and enzyme-bound reduced flavin oxidation (k_7). The small size of $^{\text{D}}V$, relative to either $^{\text{D}}V/K_{\text{pro}}$ or any reasonable value for $^{\text{D}}k_3$, requires that k_7 be less than k_3 , and that the oxidative half-reaction is the overall rate-limiting step of the two chemical steps.

To investigate the involvement of proton transfer steps occurring in the reactions, solvent KIEs were measured at pH 8.1, a region where the kinetic parameters are not changing as a result of the isotopic composition of the solvent. At saturating concentrations of DCPIP and variable concentrations of *L*-proline, SKIE's for $^{\text{D}_2\text{O}}V$ of 1.3 ± 0.1 and for $^{\text{D}_2\text{O}}V/K_{\text{pro}}$ of 2.1 ± 0.4 were determined (Figure 4B). A viscosity control using 9% glycerol to mimic the relative viscosity of D_2O was conducted, and no effect of viscosity on the rate was observed (data not shown). In order to determine the number of protons involved in the solvent isotope-dependent step, a proton inventory experiment was performed (Figure 4C). $^{\text{D}_2\text{O}}V/\text{H}_2\text{O}V$ was determined in 10% increments between 0 and ~100% D_2O . The observed linear proton inventory is indicative of a single solvent-derived proton involved in the step that is solvent sensitive. Similar to the case of primary KIE's on V/K_{pro} , only those steps involving proton transfer in the first half-reaction influence the magnitude of $^{\text{D}_2\text{O}}V/K_{\text{pro}}$. The oxidation of *L*-proline requires both a deprotonation of the secondary amine nitrogen of *L*-proline (by K110), and the transfer of a hydride ion from C5 to the N5 position of FAD. The deprotonation step will be sensitive to solvent isotopic composition, and the magnitude of $^{\text{D}_2\text{O}}V/K_{\text{pro}}$ is relatively small (2.0), suggesting that it is not rate-limiting, at least compared to the hydride transfer step reported on by the primary KIE ($^{\text{D}}V/K_{\text{pro}} = 5.5$). The magnitude of $^{\text{D}_2\text{O}}V$ suggests that cleavage of the N5-D flavin bond of reduced FAD is similarly not rate-limiting in the oxidative half-reaction.

In order to probe the stepwise versus concerted nature of *L*-proline oxidation, the primary kinetic isotope effect on *L*-proline and [2,5,5- $^2\text{H}_3$]-*L*-proline oxidation was determined in D_2O . The measured value of $^{\text{D}}V_{\text{D}_2\text{O}}$ was 1.5 ± 0.1 while $^{\text{D}}V/K_{\text{pro-D}_2\text{O}}$ was 3.4 ± 0.4 (Figure 4D). The decrease in the primary V/K KIE from 5.5 in H_2O to 3.4 in D_2O argues that the proton and hydride transfer steps are uncoupled, and that the reaction precedes via an initial deprotonation of the protonated ring nitrogen of *L*-proline ($\text{pK} = 10.6$) by K110, followed by hydride transfer from the C5 position of *L*-proline to FAD resulting in the formation of Δ^1 -pyrroline-5-carboxylate [17, 18].

Pre-Steady State Kinetic Isotope Effects

In order to confirm our interpretations of the steady-state isotope effects, we measured the rate of the individual first half-reaction, the reduction of flavin, using single turnover stopped-flow techniques. Using *L*-proline, a k_{red} rate of $88.5 \pm 0.7 \text{ s}^{-1}$ was measured with an apparent K_{d} of $33.5 \pm 0.5 \text{ mM}$. This k_{red} is ~3-fold faster than that of the ProDH from *E. coli* [14]. The k_{red} was then measured using $[2,5,5\text{-}^2\text{H}_3]$ -*L*-proline as the substrate, allowing for the calculation of the primary kinetic isotope effect on $^{\text{D}}k_{\text{red}}$ of 5.2 (Figure 5A). These data confirm that *L*-proline is not “sticky” and that the forward commitment factor is near zero. It also confirms our interpretation, based on the much smaller magnitude of the determined steady-state values of $^{\text{D}}V$ compared to $^{\text{D}}V/K_{\text{pro}}$, that oxidation of the reduced flavin by DCPIP is slower than flavin reduction by *L*-proline. For a ping-pong mechanism the reciprocal of the k_{cat} is equal to the sum of the reciprocal rates of the two half-reactions ($1/k_{\text{cat}} = 1/k_{\text{red}} + 1/k_{\text{ox}}$). Using values of $k_{\text{cat}} = 33 \text{ sec}^{-1}$ and $k_{\text{red}} = 88 \text{ sec}^{-1}$, the rate of k_{ox} can be calculated as 52 sec^{-1} . Finally, k_{red} was then measured in H_2O and D_2O yielding a $^{\text{D}_2\text{O}}k_{\text{red}}$ of 1.1, again confirming the steady-state data (Figure 5B).

Chemical Mechanism

Various mechanisms have been proposed for the oxidation of amines by flavoproteins [19, 20]. However, the mechanism of *L*-proline oxidation by ProDH is different in two significant ways: oxidation occurs at a secondary amine and oxidation involves the N1-C5 bond rather than the typical N1-C α bond. For years, the mechanism of D-amino acid oxidase (DAAO) was thought to involve base abstraction of the α -hydrogen, to form a carbanion, with the subsequent formation of the N1-C α double bond after hydride transfer to FAD [21] (Scheme 3A, shown for alanine). More recent work on various amino acid oxidases have led to an alternative mechanism in which the amino hydrogen is removed first, followed by either a concerted hydride transfer (Scheme 3B) or a step-wise transfer [17, 18, 22] (Scheme 3C). Based on our results reported here, most importantly the multiple kinetic isotope effects, we propose a mechanism for the reductive half-reaction (Scheme 3C). After *L*-proline enters the active site, it interacts with Y203, positioning it to allow for interaction of the amino ring nitrogen and the uncharged K110. Deprotonation of the ring nitrogen by K100 gives the neutral amino acid, which then collapses with donation of a hydride ion from C5 to the FAD. The proton transfer step is less energetically difficult than the hydride transfer step, as supported by our observation of a modest SKIE but a very large primary KIE on V/K_{pro} . It is this later step that is rate-limiting in the reductive half-reaction, but it is reduced flavin reoxidation that is rate-limiting for the overall reaction. This same stepwise chemical mechanism has recently been proposed for the D-arginine dehydrogenase reaction using similar isotopic approaches [24].

Acknowledgments

This work was supported by the National Institutes of Health Grants AI33696 and AI60899 to J.S.B and support for H.S. from the Geographic Medicine and Emerging Infections Training Grant NIH-NIAID T32 AI046985 awarded to the Albert Einstein College of Medicine

Abbreviations

DTT	dithiothreitol
LB	Luria broth
MES	2-(N-morpholino)ethanesulfonic acid
Ni-NTA	nickel nitriloacetic acid

PCR	polymerase chain reaction
SDS-PAGE	sodium dodecyl sulfate–polyacrylamide gel electrophoresis
Tris	tris(hydroxymethyl)aminomethane
WT	wild type
FAD	flavin adenine dinucleotide
Bis-tris propane	1,3-bis(tris(hydroxymethyl)methylamino)propane
CHES	N-Cyclohexyl-2-aminoethanesulfonic acid

References

1. Global tuberculosis report. 2012. http://www.who.int/tb/publications/global_report/en/
2. The Stop TB Strategy. 2006. <http://www.who.int/tb/strategy/en/>
3. Berney M, Cook GM. Unique flexibility in energy metabolism allows mycobacteria to combat starvation and hypoxia. *PLoS One*. 2010; 5:e8614. [PubMed: 20062806]
4. Berney M, Weimar MR, Heikal A, Cook GM. Regulation of proline metabolism in mycobacteria and its role in carbon metabolism under hypoxia. *Mol Microbiol*. 2012; 84:664–681. [PubMed: 22507203]
5. Casazza JP, Felver ME, Veech RL. The metabolism of acetone in rat. *J Biol Chem*. 1984; 259:231–236. [PubMed: 6706932]
6. Dhar A, Desai K, Kazachmov M, Yu P, Wu L. Methylglyoxal production in vascular smooth muscle cells from different metabolic precursors. *Metabolism*. 2008; 57:1211–1220. [PubMed: 18702946]
7. Huang TC, Huang YW, Hung HJ, Ho CT, Wu ML. Delta1-pyrroline-5-carboxylic acid formed by proline dehydrogenase from the *Bacillus subtilis ssp. natto* expressed in *Escherichia coli* as a precursor for 2-acetyl-1-pyrroline. *J Agric Food Chem*. 2007; 55:5097–5102. [PubMed: 17536821]
8. Nemet I, Turk Z, Duvnjak L, Car N, Varga-Defterdarovic L. Humoral methylglyoxal level reflects glycemic fluctuation. *Clin Biochem*. 2005; 38:379–383. [PubMed: 15766739]
9. Weber J, Kayser A, Rinas U. Metabolic flux analysis of *Escherichia coli* in glucose-limited continuous culture. II. Dynamic response to famine and feast, activation of the methylglyoxal pathway and oscillatory behaviour. *Microbiology*. 2005; 151:707–716. [PubMed: 15758217]
10. Tanner JJ. Structural biology of proline catabolism. *Amino Acids*. 2008; 35:719–730. [PubMed: 18369526]
11. Moxley MA, Tanner JJ, Becker DF. Steady-state kinetic mechanism of the proline:ubiquinone oxidoreductase activity of proline utilization A (PutA) from *Escherichia coli*. *Arch Biochem Biophys*. 2011; 516:113–120. [PubMed: 22040654]
12. White TA, Krishnan N, Becker DF, Tanner JJ. Structure and kinetics of monofunctional proline dehydrogenase from *Thermus thermophilus*. *J Biol Chem*. 2007; 282:14316–14327. [PubMed: 17344208]
13. Zhang M, White TA, Schuermann JP, Baban BA, Becker DF, Tanner JJ. Structures of the *Escherichia coli* PutA proline dehydrogenase domain in complex with competitive inhibitors. *Biochemistry*. 2004; 43:12539–12548. [PubMed: 15449943]
14. Moxley MA, Becker DF. Rapid reaction kinetics of proline dehydrogenase in the multifunctional proline utilization A protein. *Biochemistry*. 2012; 51:511–520. [PubMed: 22148640]
15. Ho SN, Hunt HD, Horton RM, Pullen JK, Pease LR. Site-directed mutagenesis by overlap extension using the polymerase chain reaction. *Gene*. 1989; 77:51–59. [PubMed: 2744487]
16. Czekster CM, Vandemeulebroucke A, Blanchard JS. Kinetic and Chemical Mechanism of the Dihydrofolate Reductase from *Mycobacterium tuberculosis*. *Biochemistry*. 2011; 50:367–375. [PubMed: 21138249]
17. Gaweska HM, Roberts KM, Fitzpatrick PF. Isotope effects suggest a stepwise mechanism for berberine bridge enzyme. *Biochemistry*. 2012; 51:7342–7347. [PubMed: 22931234]

18. Fan F, Gadda G. On the catalytic mechanism of choline oxidase. *J Am Chem Soc.* 2005; 127:2067–2074. [PubMed: 15713082]
19. Fitzpatrick PF. Insights into the mechanisms of flavoprotein oxidases from kinetic isotope effects. *J Labelled Comp Radiopharm.* 2007; 50:1016–1025. [PubMed: 19890477]
20. Fitzpatrick PF. Oxidation of amines by flavoproteins. *Arch Biochem Biophys.* 2010; 493:13–25. [PubMed: 19651103]
21. Ghisla S, Massey V. Mechanisms of flavoprotein-catalyzed reactions. *Eur J Biochem.* 1989; 181:1–17. [PubMed: 2653819]
22. Sobrado P, Fitzpatrick PF. Solvent and primary deuterium isotope effects show that lactate CH and OH bond cleavages are concerted in Y254F flavocytochrome b2, consistent with a hydride transfer mechanism. *Biochemistry.* 2003; 42:15208–15214. [PubMed: 14690431]
23. Luo M, Arentson BW, Srivastava D, Becker DF, Tanner JJ. Crystal structures and kinetics of monofunctional proline dehydrogenase provide insight into substrate recognition and conformational changes associated with flavin reduction and product release. *Biochemistry.* 2012; 51:10099–10108. [PubMed: 23151026]
24. Yuan H, Xin Y, Hamelberg D, Gadda G. Insights into the mechanism of amine oxidation by D-arginine Dehydrogenase through pH and kinetic isotope effects. *J Am Chem Soc.* 2011; 133:18957–18965. [PubMed: 21999550]

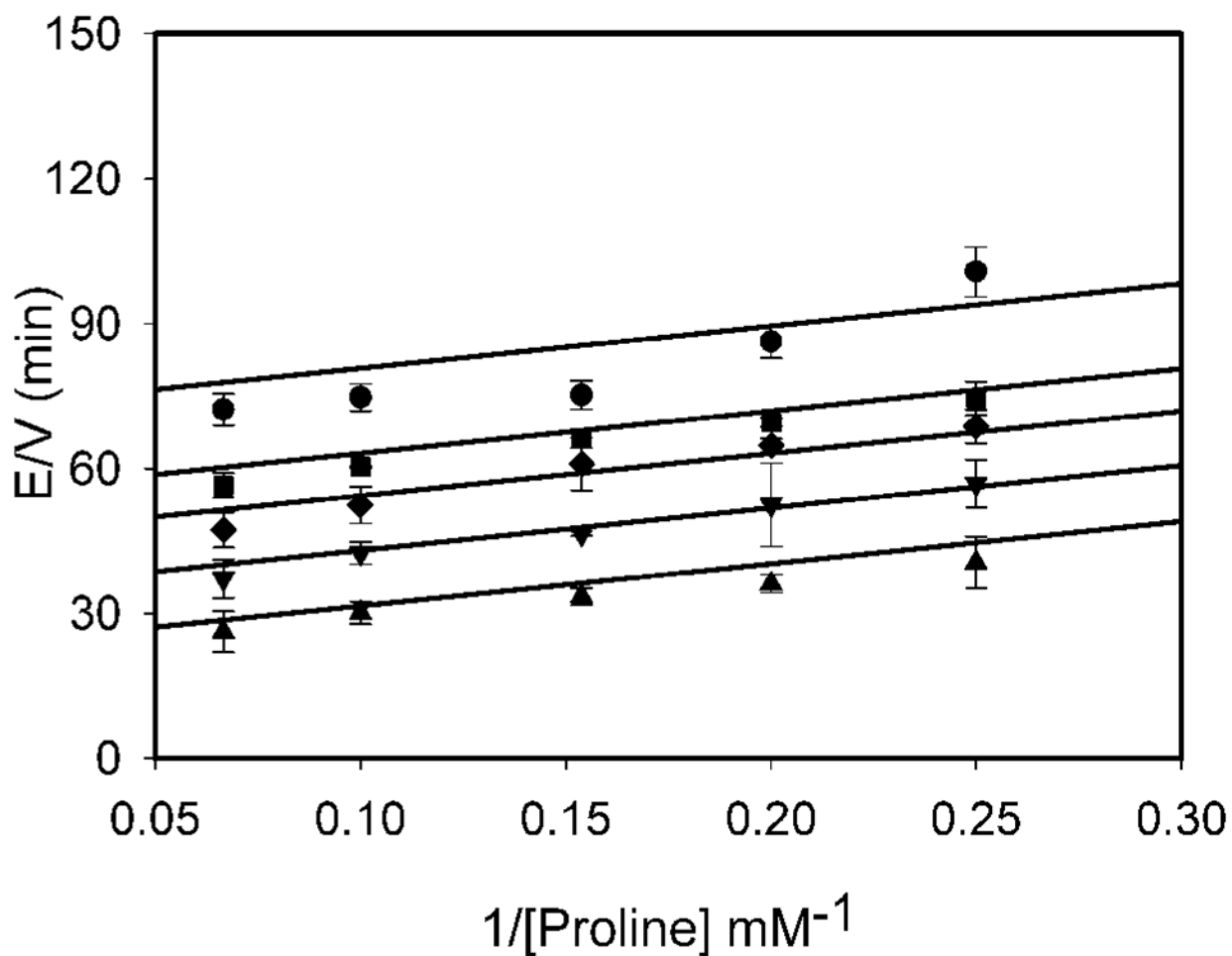


Figure 1.

Bisubstrate kinetic analysis of ProDH. The initial velocity of proline oxidation was measured in 50 mM Tris-HCl (pH 7.4) with varying concentrations of L-proline (4-15 mM) and fixed concentrations of DCPIP: 1 (●), 1.5 (■), 2 (◆), 3.5 (▼), and 15 μ M (▲). Shown is the double-reciprocal plot of the initial velocity as a function of DCPIP concentrations. Global fitting of the data to eq 2 (solid lines) gave a k_{cat} of $33 \pm 2 \text{ sec}^{-1}$, a $K_{\text{L-pro}}$ of $5.7 \pm 0.8 \text{ mM}$, and a K_{DCPIP} of $3.4 \pm 0.3 \mu\text{M}$.

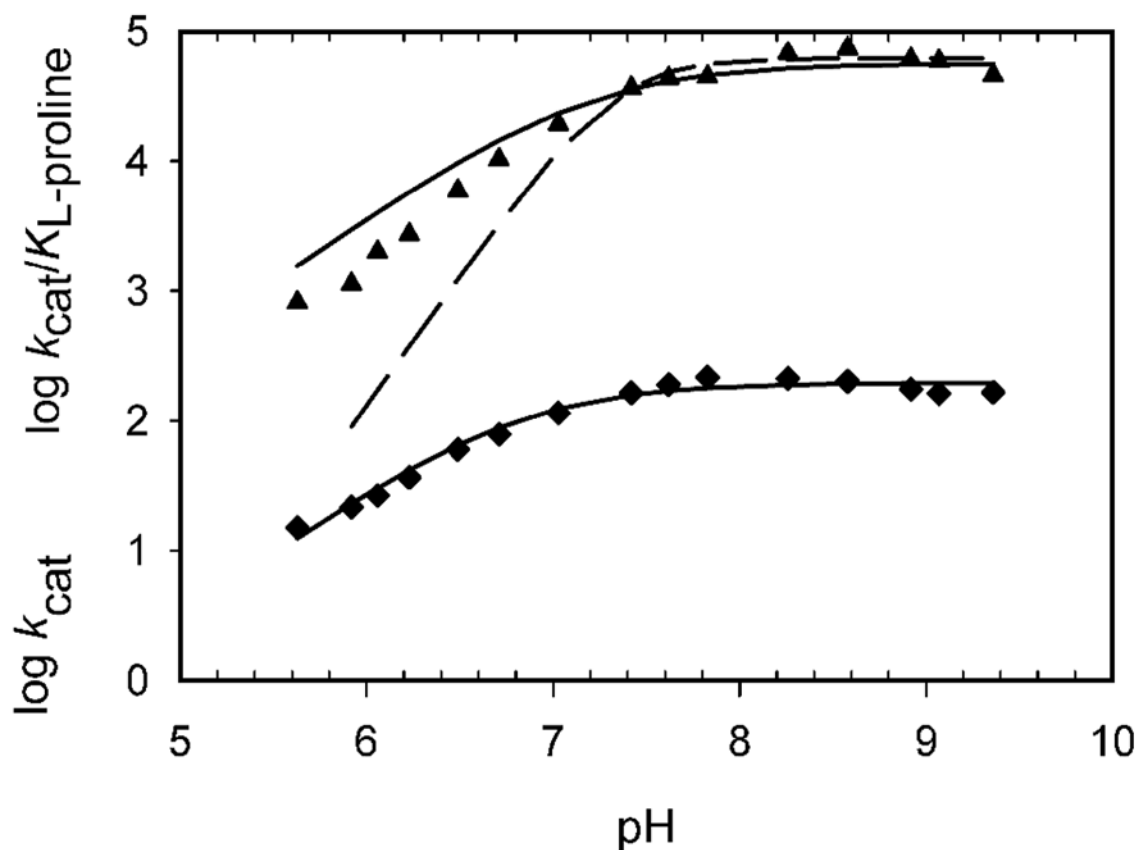


Figure 2. pH dependence of ProDH. $k_{cat}(\text{app})$ (●) and $k_{cat}/K_{L\text{-pro}}(\text{app})$ (▲), determined at saturating DCPIP and varying L-proline concentrations. The solid lines are fits to eq 3, yielding a pK_a of 6.8 ± 0.1 for $k_{cat}(\text{app})$ and 7.1 ± 0.2 for $k_{cat}/K_{L\text{-pro}}(\text{app})$. The dashed line in the $k_{cat}/K_{L\text{-pro}}$ pH profile represents a fit where two groups must be deprotonated.

```

D. radiodurans  ADDVIKLI EAAHAAGI-----KPYVSIKLSVGGQK DENGEDLGLTNAR----RIIAK 124
T. thermophilus  QRGLLELVWALAGKPW-----PKYISLKLTLQLGLDLS---EDLALALLR----EVLRE 122
M. tuberculosis  VRAYLGLLDVLGRRGDIACDGV RPLEVSLKLSALGQALDRD GQKIALDNAR----AICER 136
M. smegmatis     VAAYLALLEGLKSDSD---AKVRPLEVSLKLSALGQALPRD GEKIALENAH----TICAK 132
E. coli          MVSYQQAIHAIGKASN-GRGIYEGPGISIKLSALHP RYSRAQYDRVMEELYPRLKSLTLL 359
                :                               :*:** :           . :           :

D. radiodurans  AKEYGGFICLDMEDHTRVDVTLEQFRTL VGE---FGAEHVGTVLQSYLYRS-----LGD 175
T. thermophilus  AEPRGVFVRLDMEDSPRVEATLR LYLALR-E---EGFSQVGI VLSYLYRT-----EKD 172
M. tuberculosis  AERVGAWVTVDAEDHTTTDSTLSISGD LR-----VDFPWLGT VVQAYLRRT-----LAD 185
M. smegmatis     ARDIEAWVTVDAEDHTTTDSTLSI VRDLR-----TEFDWLGT VLQAYLKRT-----RAD 181
E. coli          ARQYDIGINIDAEADRLEISLDLLEKLC FEPELAGWNGIGFVIQAYQKRCPLVIDYLID 419
                *.           : :* *:           : :*           *           :* **:* * *           *

D. radiodurans  RASLDDL RPNIRMVKGAYLE-----PATVAYPDKADVDQ NYRRLVFQHLKAG-- 222
T. thermophilus  LLDLLPYRPNLRLVKGAYRE-----PKEVAF PDKRLIDAEYLHLGKLALKEG-- 219
M. tuberculosis  CAELA AVGARVRLCKGAYDE-----PASVAYRDA AQVTD SYLRCLRVLTAGR-- 232
M. smegmatis     CAEFAASGARIRLCKGAYDE-----PASVAYRDP DEVTDSYLTCLRILMAGR-- 228
E. coli          LATRSRRRLMIRLVKGAYWDSEIKRAQMDGLEGPVYTRK VYTDVSYLACAKKLLAVPNL 479
                :*: **** :                               .:           .*

```

Figure 3. Sequence alignment of ProDH from various organisms. Highlighted are the two residues believed to play a role as the general base.

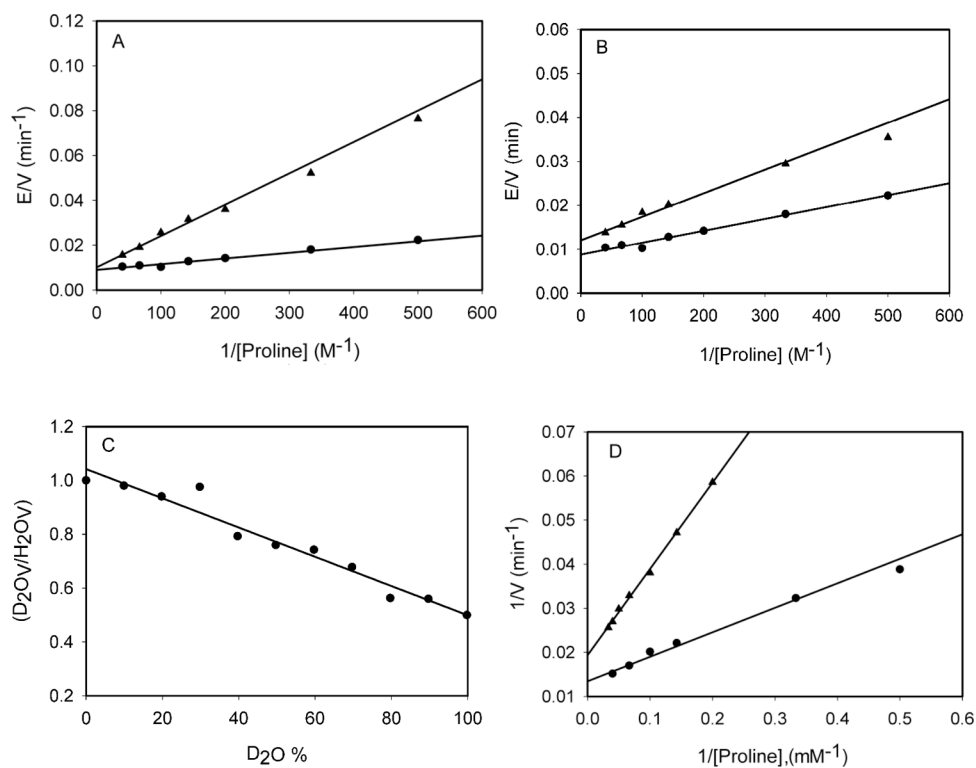


Figure 4.

Kinetic isotope effects. (A) Primary kinetic isotope effects at saturating DCPIP (80 μ M) and varying (2 – 25 mM) L-proline (●) or [2,5,5-²H₃]-L-proline (▲) concentrations at pH 8.05. Data was fit to eq 4, which gave a ^DV of 1.1 ± 0.2 and a ^DV/ K_{L-pro} of 5.6 ± 0.1 . (B) Solvent kinetic isotope effects at saturating DCPIP (80 μ M) and varying (2 – 25 mM) L-proline concentrations in H₂O (●) or D₂O (▲) at pH 8.05. Data was fit to eq 4, which gave a ^DV of 1.3 ± 0.1 and a ^DV/ K_{L-pro} of 2.1 ± 0.4 . (C) Proton inventory at saturating DCPIP (80 μ M) and saturating L-proline (20 mM) concentrations at pH 8.05 in 10% D₂O increments from 0 to 100% (D) Primary kinetic isotope effects at saturating DCPIP (80 μ M) and varying (2 – 25 mM) L-proline (●) or (5 – 25 mM) [2,5,5-²H₃]-L-proline (▲) concentrations performed in D₂O at pH 8.05. Data was fit to eq 4, which gave a ^DV of 1.5 ± 0.1 and a ^DV/ K_{L-pro} of 3.4 ± 0.4 .

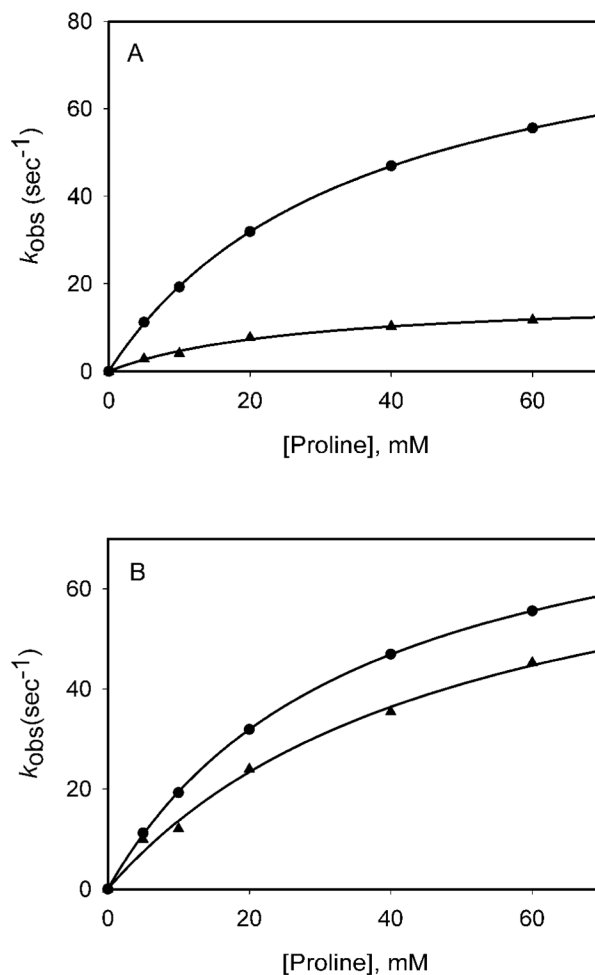
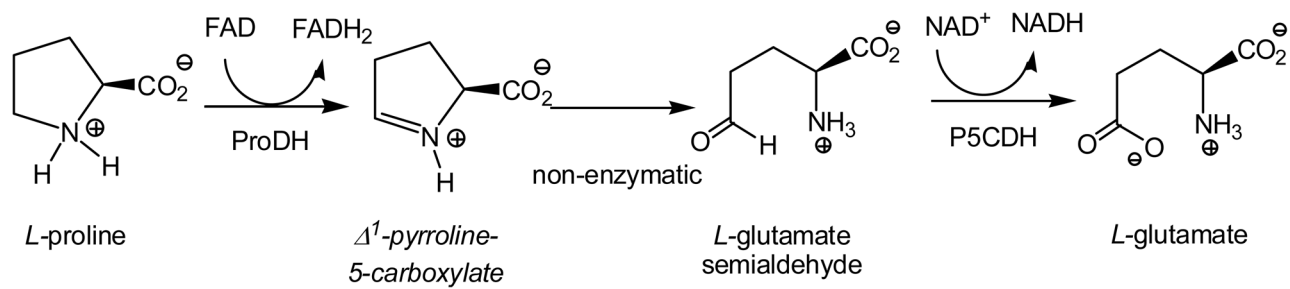
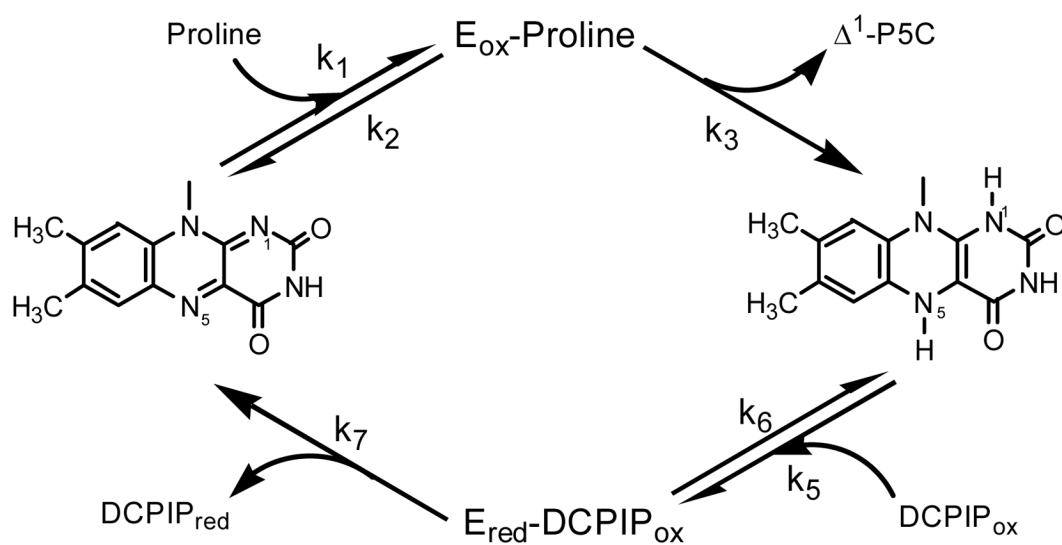


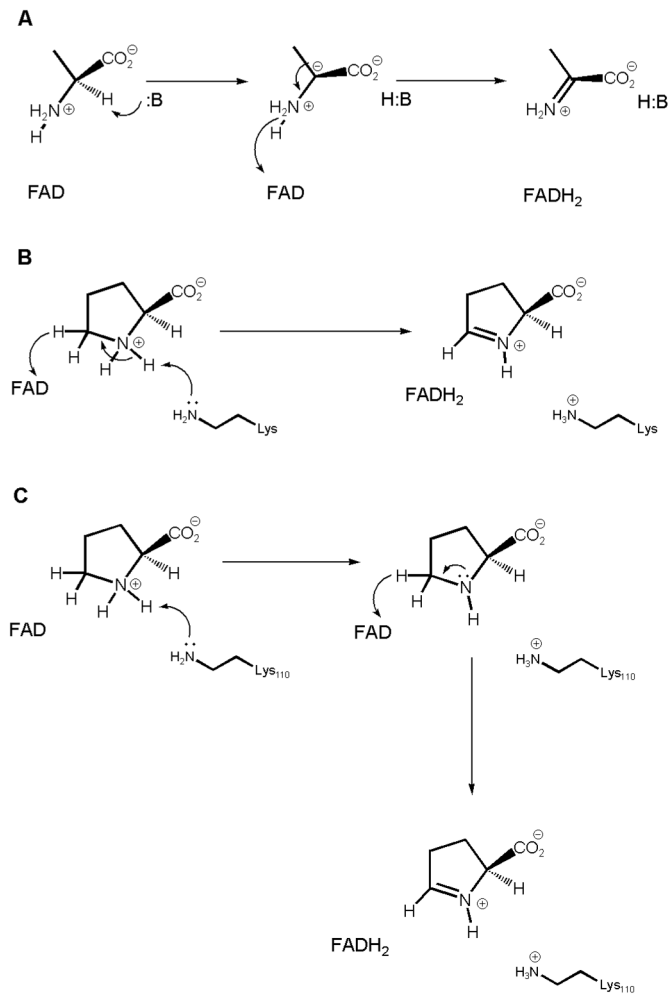
Figure 5. Stopped-flow Kinetic Isotope Effects. (A) Primary KIEs. Each point represents the average of three traces collected with 14 μM ProDH and various concentrations of L-proline (●) or [2,5,5- $^2\text{H}_3$]-L-proline (▲) (5–60 mM) (B) Solvent KIEs. Each point represents the average of three traces collected with 14 μM ProDH and various concentrations of L-proline (5–60 mM) in H_2O (●) or D_2O (▲).



Scheme 1.



Scheme 2.



Scheme 3.

Table 1Kinetic Parameters for ProDH and the Y203F Mutant^a

enzyme	k_{cat} (sec ⁻¹)	K_{DCPIP} (μM)	K_{pro} (mM)	$k_{\text{cat}}/K_{\text{pro}}$ (M ⁻¹ sec ⁻¹)
ProDH	33.5 \pm 2.2	3.4 \pm 0.3	5.7 \pm 0.8	5877
Y203F	100.6 \pm 2.1	ND ^b	860 \pm 31	117

^aThe steady-state kinetic parameters were measured in 20 mM tris-HCl buffer (pH 7.1) at 25 °C. Errors are standard deviations. Substrate concentrations are described in the Methods section.

^bNot determined